R. Vescovini, C. Bisagni
A Fast Procedure for the Design of Composite Stiffened Panels
Aeronautical Journal, Vol. 119, N. 1212, 2015, p. 185-201

A Fast Procedure for the Design of Composite Stiffened Panels

Riccardo Vescovini, Chiara Bisagni*

Dipartimento di Scienze e Tecnologie Aerospaziali, Politecnico di Milano

Via La Masa 34, 20156 Milano, Italy

Abstract

This paper describes the analysis and the minimum weight optimization of a fuselage composite stiffened panel made from carbon/epoxy material and stiffened by five omega stringers. The panel investigated inside the European project MAAXIMUS is studied using a fast tool, which relies on a semi-analytical procedure for the analysis and on genetic algorithms for the optimization. The semi-analytical approach is used to compute the buckling load and to study the post-buckling response. Different design variables are considered during the optimization, such as the stacking sequences of the skin and the stiffener, the geometry and the cross-section of the stiffener. The comparison between finite element and fast tool results reveals the ability of the formulation to predict the buckling load and the post-buckling response of the panel. The reduced CPU time necessary for the analysis and the optimization makes the procedure an attractive strategy to improve the effectiveness of the preliminary design phases.

Keywords: stiffened panel, composite materials, optimization, analytical methods.

Nomenclature

a	panel length
b	width of the skin
fit	fitness function
K_{pre}, $K_{\text{pre}}^{\text{ref}}$	pre-buckling stiffness and pre-buckling stiffness reference value

Presented at the 3^{rd} Aircraft Structural Design Conference, Structures & Materials Group Conference, Royal Aeronautical Society, 9-11 October 2012, Delft, The Netherlands.

*Corresponding author. *Email address:* chiara.bisagni@polimi.it (Chiara Bisagni)

N_c	number of constraints
N_{cp}	number of consecutive plies with the same angle of orientation
N_{dp}	number of violations of the disorientation constraint
P_{buck}, $P_{\text{buck}}^{\text{ref}}$	buckling load and buckling load reference value
W, W^{ref}	structural weight and structural weight reference value
Y_k, Y_k^{ref}	structural constraint and structural constraint reference value
α	scalar coefficient for the penalty term
γ_{tech}	scalar coefficient for the technological requirements
Δ	constraint violation
θ	angle between the stiffener lateral web and the normal to the skin
ν	equivalent Poisson's ratio of the laminate
ξ_k	penalty function for the generic constraint k
ξ_{cp}	penalty function for the constraint regarding the number of consecutive plies
ξ_{dp}	penalty function for the disorientation constraint
ξ_{pm}	penalty function for the Poisson's mismatch constraint

1 Introduction

The design of modern aeronautical structures is usually conducted by analyzing models with different levels of complexity. Referring to the design of a composite fuselage, the highest level of complexity is represented by the complete structure, i.e. the overall fuselage. At this level, the virtual testing of the structure is performed making use of refined models, where a detailed representation of the structure including frames, stiffeners, cut-outs, reinforcements, and joints is needed. In most cases, this phase is conducted with a finite element approach. However, the high number of degrees of freedom makes this level of complexity computationally expensive. This aspect becomes particularly true if several analyses are needed, such as in the case of sensitivity analyses or design optimizations.

Simpler models can be achieved by considering portions, which can be of different dimensions, of the complete fuselage. Two examples are the full size and the subdomain panels. In general, these panels are more suitable to perform numerical analyses, and even the realization of an experimental test is less costly if compared to a full scale test. Examples are found in the works of Lynch et al. [1] and Linde et al. [2], where the post-buckling behaviour of aeronautical fuselage panels is assessed referring to the finite element method. Despite the ability of the method to effectively handle complex geometries and various kinds of bound-

ary and loading conditions, the computational effort to realize sensitivity studies and design optimization can be quite high, especially when repeated eigenvalue and nonlinear analyses are needed. Indeed, the typical size of the panel finite element model is of the order of hundreds of thousands of degrees of freedom. In this case, linear static analyses can be performed relatively quickly. In the case of post-buckling analyses, the problem is characterized by a higher number of operations and potential convergence issues due to mode jumpings, snap-backs or snap-throughs. For this reason, different techniques were developed with the aim of reducing the computational effort to perform buckling and post-buckling analyses. A multi-scale approach is found in [3], and is based on Schur non-overlapping decomposition of the structure and Krylov solvers, in the context of a Newton-Raphson scheme. An improved version of the method is developed for problems characterized by local nonlinearities, as in the case of local skin buckling, by Cresta et al. [4].

An efficient strategy is the model reduction technique [5, 6], where the nodal displacement vector is described as the linear superposition of a small number of basis vectors, so allowing a reduction of the number of the finite element equations. An advanced approach based on the projection-based model reduction is proposed in [7], where the post-buckling state is represented as the superposition of a linear pre-buckling state and higher order variation terms. Another approach to improve the computational efficiency is represented by the analytical and semi-analytical methods. In general, they are based on the analysis of a small portions of structure, taken as representative of the behaviour of the overall fuselage panel. The use of these units is justified by the fact that the fuselage can be thought as a periodic structure, making appropriate the analysis of the repeating unit only. Typical models at this level complexity are the portion of skin between two stiffeners, which can be constrained along the edges with various boundary conditions or the portion of structure including the skin and the stiffeners.

Some formulations consider the panel, without the stiffeners, subjected to simply-supported or clamped conditions [8–11].

Analytical approaches are found also for panels subjected to elastically restrained boundary conditions, where the elasticity of the boundary conditions accounts for the effect of the stiffener [12–14]. Other analytical strategies model the stiffeners using a plate element representation. Most of these approaches are limited to the case of isotropic materials [15–18], while quite a few works are found regarding the composite panels [19, 20].

With regards to the preliminary optimization of composite structures, the computational costs become a crucial aspect. In many cases, efficiency is achieved making use of surrogate methods in conjunction with optimization strategies, such as in the works of Bisagni and

Lanzi [21] and Murugan et al. [22] . On the other hand, the use of analytical and semi-analytical techniques as analysis tool is still quite limited. Examples are found in the work of Bushnell [23], where the program PANDA2 is used together with gradient based optimization techniques, and in the work of Kennedy and Featherston [24] that presented a mass minimization procedure based on the coupled use of the Wittrick-Williams algorithm and gradient-based tools. Diaconu and Weaver [25] developed approximate solution for infinitely long and symmetrically laminated composite plates in the context of an optimization based on the use of lamination parameters. Herencia and Weaver [26] applied analytical closed-form solutions to evaluate the buckling load of infinitely long panels, and performed the optimization using genetic algorithms. Bisagni and Vescovini [20] applied a semi-analytical method to perform buckling and post-buckling computations, using genetic algorithms for the optimization.

This paper presents part of the activity performed by Politecnico di Milano during the MAAXIMUS (More Affordable Aircraft structure through eXtended, Integrated, & Mature nUmerical Sizing) project [27]. The work regards the development of a fast computational procedure for the buckling and post-buckling analysis of composite stiffened panels at the representative unit level. The proposed tool offers the advantage of allowing the study of a relatively wide set of configurations, including composite and isotropic materials, flat and curved panels, and combined loading conditions. Compared to other approaches in literature, where the skin of the panel is conservatively assumed as simply-supported, the proposed analysis tool is able to account for stiffener elasticity and, eventually, to capture local stiffener buckling. The analysis and the optimization of the MAAXIMUS Use Case panel, consisting of a top fuselage panel made from carbon/epoxy material and stiffened by five omega stringers, is discussed. The panel is studied by identifying a representative unit and using the semi-analytical formulation presented in two previous works by the authors [20, 28]. The comparison with finite element results is presented in terms of buckling load, post-buckling out of plane displacements and stress distributions. Finally, an optimization of the panel is presented to minimize the weight of the panel under structural requirements and design recommendations.

2 Fast design procedure

The fast procedure is developed to allow the preliminary design of composite stiffened panels under buckling and post-buckling requirements. Structural phenomena such as crippling and stiffener debonding are not here considered. Indeed, their evaluation could be hardly

performed in the context of a semi-analytical approach. In the present paper, loading conditions of pure compression are considered, even though the formulation can handle combined conditions of compression and shear. The procedure relies on the assumption of symmetric and balanced laminate, and applies the classical lamination theory [29, 30].
The design tool is divided into two main parts, implemented in Matlab language, which are the analysis and the optimization modules. The first module has the goal of allowing fast structural analyses with regard to the buckling and the post-buckling behaviour. It can be used during the design phase to study the response of a given configuration or in the context of an optimization loop. In this second case, it is linked to the optimization module, which is based on genetic algorithms.

2.1 Semi-analytical formulations

The analysis module is divided into two different semi-analytical formulations, as summarized in Table 1. The two formulations are developed to study a multi-stiffener panel as the one of Fig. 1(a).
The first of the two formulations is based on the use of a representative unit composed of two stiffeners, one bay and two half-bays. In this case, the panel is represented by means of plate elements, which are used to model the skin and the stiffener, as sketched in Fig. 1(b). The plate representation guarantees an accurate description of the interaction between the skin and the stiffener, and allows to capture the skin buckling as well as the local stiffener instabilities. The problem is formulated referring to the minimum potential energy principle and the method of Ritz. The method allows to perform the linear buckling analysis, and the governing equations are written in the form of a standard eigenvalue problem. Typical dimensions of the problems are of the order of few hundreds of degrees of freedom, so leading to a quick solution of the governing problem.
The second formulation is developed for the post-buckling analysis. In this case, the model is further simplified, and considers the skin between two stiffeners. A sketch of the structural model is provided in Fig. 1(c). For efficiency, the stiffener is modeled by means of torsion springs whose stiffness is derived from the buckling load computed with the plate assembly model. The formulation is capable of describing the nonlinear response of the panel, not necessarily limited to the initial post-buckling range. The nonlinear governing equations are solved with an arc-length procedure [16] in order to allow the identification of possible mode-jumping and snap-back responses. Indeed, these phenomena often characterize the post-buckling field [31] and cannot be captured by a standard Newton-Raphson iteration

scheme.

The semi-analytical model is used to trace the force-displacement curve, and to plot the deformed configuration at different load levels, as well as the contour of the stresses on the different plies of the skin.

2.2 Optimization algorithm

The optimization module is based on genetic algorithms, here implemented thanks to their ability to handle design spaces characterized by local optima. Furthermore, they allow the handling of non-smooth design spaces and offer the possibility of considering both continuous and discrete design variables. For these reasons, genetic algorithms were successfully applied to the optimization of composite structures in several works [32–34]. The main drawback, consisting in the high number of required objective function evaluations, is here overcome by the coupling of the computationally efficient semi-analytical structural analysis formulation.

The present implementation considers a division of the chromosomes into sub-strings, each one characterized by an alphabet of arbitrary cardinality according to the nature of the design variable. Alphabets of cardinality n can be adopted to encode the lay-ups, while the binary alphabet is used for geometric quantities.

The initial population is created with a random initialization of the chromosomes, where any of the sub-strings is initialized according to the cardinality of the chosen alphabet.

After the fitness evaluation of all the members of the population, the selection of the parents is performed with a procedure based on the tournament method and an arbitrary number of competitors. The algorithm implements an elitist selection, in order to guarantee that the fitness function cannot decrease during the iterations.

The genetic operators, i.e. crossover and mutation, are developed by implementing the modifications proposed by Nagendra et al. [32]. In particular, a modified version of one-point crossover is implemented, and six different mutation operators are used. They are bit flip, ply addition, ply deletion, intra-laminar swap, inter-laminar swap and ply angle mutation [32].

The iterative procedure is repeated until the objective function of the fittest individual is not increased within a maximum number of generations.

3 Use Case panel

The MAAXIMUS Use Case panel is representative of a top fuselage panel and is illustrated in Fig. 2. It consists of a curved panel with five omega stiffeners. The total length is 2500

mm, and the width is 893 mm. Three bays with length equal to 587.5 mm are delimited by the frame lines, whose effect is to constrain the displacement along the out of plane direction. The height of the omega stiffener is equal to 24 mm, while the width of the crown is equal to 27 mm. The portion of skin under the stiffener is 36 mm long, while the skin pad-up has a maximum width of 22 mm, and is obtained by enlarging the flange to allow the riveting of the frame. Details of the stiffener geometry are reported in Fig. 3.

The panel is made from M21E/IMA carbon fiber prepreg and is laminated with symmetrical stacking sequences. The material elastic properties and the ply strengths are reported in Tables 2 and 3 In particular, the skin has a quasi-isotropic lay-up $[\pm 45°/0°/90°/\mp 45°]_s$, while the stiffener has lay-up $[45°/0°/-45°/0°/90°/0°/-45°/0°/45°]$.

A preliminary finite element analysis is performed on the complete Use Case panel in order to investigate its buckling behaviour, and to obtain a benchmark solution to be used for successive comparisons.

The analyses are performed using the commercial code Abaqus [35]. The finite element model is realized with S4R shell elements, thanks to the performances in terms of accuracy and computational time due to the reduced integration. The mesh size, of approximately 6 $\times$ 6 mm, is chosen on the basis of a preliminary convergence analysis. It is characterized by 20 elements from stiffener to stiffener along the transverse direction, and 844 elements along the longitudinal direction. The total number of degrees of freedom is 522828.

The skin and the stiffener are modeled using one shell element in the thickness direction. Similarly, the lay-up obtained from the stacking of the skin and the stiffener together with a proper offset is assigned to the elements in the skin pad-up region.

The panel is fixed at one end by constraining all the degrees of freedom. The other end of the panel is fixed except for the translation along the axial direction. The longitudinal edges are free to translate along the transverse direction, while the three rotations and the out of plane displacements are constrained. The panel is also constrained to exhibit null out of plane displacement in correspondence of the frame lines.

A linear static analysis is firstly performed to determine the pre-buckling stiffness, resulting equal to 59.2 kN/mm. From the linear eigenvalue analysis, a buckling load of 258.4 kN is obtained, while the corresponding axial displacement is 4.4 mm. The first buckling mode, as shown in Fig. 4, is characterized by a local skin instability in the central bay. The results of the buckling eigenvalue analysis reveal that the first and the second eigenvalues differ by less than 0.1%. The linear combination of the first two modes is superposed to simulate the initial imperfections for the post-buckling analysis. The amplitude to thickness ratio, in absence of experimental measurements, is taken equal to 0.1 based on past experience.

The post-buckling analysis is performed using a quasi-static nonlinear analysis. The results are reported in terms of force-displacement curve in Fig. 5(a) for the full post-buckling range here considered. The deformed shape is plotted in Fig. 5(b), where the contour of the out of plane deflections is reported in proximity of the first instability.

In agreement with the results obtained from the linear buckling analysis, the deformed configuration shows a local post-buckling response. The behaviour is characterized by a local skin buckling between the stiffeners with seven halfwaves per bay along the transverse direction. At a load level of approximately 700 kN, the global buckling mode is triggered, and consequently a significant loss of stiffness is observed in the force-displacement curve.

Adopting a fist ply failure criterion based on the maximum stress and the Tsai-Hill indices, the first ply failure load is equal to 607.5 kN, corresponding to an imposed displacement of 11.6 mm.

In terms of computational time, the eigenvalue analysis required 243 minutes on a Core2 Duo 3.00 GHz with 2 GB of RAM, while the quasi-static one took more than 10 hours. It is worth noting that the time to realize the model has to be added to obtain a realistic estimate of the overall time to study the panel.

4 Analysis

The fast design tool is here applied to study the MAAXIMUS Use Case panel. The results of the previous section showed that the panel undergoes a local skin instability with a periodic pattern, as revealed from Fig. 5(b). For this reason, the semi-analytical formulation, which is based on the assumption that the study of the panel can be reduced to the study of a smaller representative unit, can be effectively applied.

4.1 Model description

The representative unit for the buckling analysis is illustrated in Fig. 1(b). In the present case, it has dimensions 587.5 $\times$ 300 mm and is loaded with an imposed axial displacement. The model to perform the post-buckling analysis is represented by the portion of skin between the stiffeners, as sketched in Fig. 1(c). The dimensions of the elastically restrained skin are 587.5$\times$ 114 mm.

These two portions of structure can be thought as the building units of an infinitely periodic structure, which is a good approximation if the structure is large, as in the case of a fuselage composed by several bays. For a panel of finite dimensions, such as in the case of the Use

Case panel, the representative unit does not account for the effect of the lateral boundary conditions. However, this is a reasonable assumption at an early design phase, and does not affect the ability of the method to identifying the effect of the various parameters on the buckling response of the structure. Another approximation that is introduced with the aim of simplifying the structural model consists in neglecting the skin pad-up. This approximation is applied both to the numerical and the analytical models.

The finite element model of the representative unit is composed of two stiffeners, one bay and two semi-bays, and is realized to provide a comparison with the semi-analytical results. The model is used to perform eigenvalue and static nonlinear analyses. The mesh is realized with S4R shell elements, and is characterized by a mesh size of dimension 6×6 mm, for a total of 42176 degrees of freedom. The dimensions of the representative unit are summarized in Fig. 6. Concerning the boundary conditions, the transverse edges of the panel are clamped, while the longitudinal edges are subjected to periodic boundary conditions to account for the effect of the surrounding structure. In particular, it is assumed that the out of plane displacement and the rotation around the longitudinal axis of the two external edges are identical. Furthermore, the edges are maintained straight, but are free to expand, so that no transverse compression is induced in the model.

4.2 Analysis results

The semi-analytical buckling calculations are performed using 10×10 shape functions to represent the out of plane deflection of the skin and 10×7 shape functions for the stiffener elements. The number of functions is chosen on the basis of a preliminary convergence analysis. The solution is computed in approximately 1 s, and a buckling load of 55.6 kN is obtained. The corresponding axial displacement is equal to 0.8 mm. The numerical buckling load obtained from the Abaqus analysis of the representative unit is 54.7 kN, and the axial displacement corresponding to the buckling condition is 0.8 mm. In this case, the analysis requires 34 s of CPU time.

The comparison between the numerical and the semi-analytical buckling mode shape is presented in Fig. 7.

The two analyses are in agreement in the identification of a local skin buckling mode, characterized by a pattern with similar lengths of the half-waves. However, it is worth observing that the numerical results display a buckling mode with 7 half-waves, while the analytical solution leads to a 6 half-waves buckling mode. This discrepancy is explained by the existence of two eigenvectors with almost coincident eigenvalues. Indeed, the difference between

the first two eigenvalues is less than 1%, both numerically and analytically.

After performing the buckling analysis, the nonlinear post-buckling response of the panel is studied. In order to avoid numerical convergence issues, an initial imperfection is introduced with a shape given by the superposition of the first two buckling modes and maximum amplitude to thickness ratio equal to 0.1. The panel is loaded with an imposed displacement equal to 2.3 mm.

The semi-analytical analysis is performed using 12×12 shape functions to represent the panel deflection, corresponding to a system of 145 nonlinear equations. In this case, the total computational time to solve the problem is approximately 15 s. The finite element analysis is performed using the Abaqus nonlinear quasi-static solution procedure with automatic stabilization, and leads to a computational time of 94 s.

The first comparison between numerical and semi-analytical results regards the force - displacement curve, and is illustrated in Fig. 8.

The comparison reveals identical results in the pre-buckling range. On the other hand, a small difference is observed in the post-buckling field, with the semi-analytical model leading to a stiffer structure with respect to the numerical one. For an imposed displacement of 2.3 mm, the semi-analytical solution predicts 137.5 kN, while the numerical one is 133 kN, corresponding to a difference of 3%.

During the initial loading phase, the numerical configuration presents a six half-wave pattern, whereas the semi-analytical one is characterized by seven halfwaves. However, just after the buckling load, the numerical model exhibits a transition to a configuration with seven halfwaves, in agreement with the shape predicted by the semi-analytical model. The comparison is reported in Fig. 9 at the end of the loading phase, when the applied displacement is equal to 2.3 mm.

The maximum stress can be used to estimate the failure load according to a first ply failure criterion, or to establish the onset of a damage propagation within the structure.

The comparison between the numerical and the semi-analytical contours is presented in Fig. 10, where the contour is reported for the ply exhibiting the highest failure index, that in this case is the first ply of the skin stacking sequence oriented at 45°. The results are reported at the end of the loading phase for an applied displacement of 2.3 mm.

The maximum stress failure index calculated analytically is 0.60, while the finite element prediction is 0.63. Good comparison is obtained also for the other plies of the skin, with a maximum percent difference between numerical and semi-analytical results below 5%. Therefore, the semi-analytical formulation can provide an accurate evaluation of the stress, offering, in addition, the possibility of automatically identifying the critical ply and the

critical area.

5 Optimization

In the second phase, the fast design tool is applied to minimize the weight of the representative unit of the Use Case panel introducing structural requirements on the axial stiffness and the buckling load. Loading conditions of compression are considered.

5.1 Design variables

In the present optimization, the panel dimensions are kept constant under the assumption that the frame and the stiffener spacing were already defined. On the other hand, the section of the omega stiffener is one of the design variables. In particular, it is decided to keep constant, and equal to 75.8 mm, the sum of the width of the crown and of the two lateral webs. On the other hand, the geometry can vary through the web angle measured from the normal to the skin, here denoted as θ. The bounds for the angle θ are $0°$ and $25°$, where $0°$ corresponds to a rectangular cross-section.

The skin and the stiffener are layered with a number of plies, which is allowed to vary between 4 and 24. Furthermore, it is assumed that the lay-ups are symmetric and the angles of orientation are restricted to $0°$, $\pm 45°$ and $90°$.

The design variables suggest the sub-division of the chromosome into three fields. The first two sub-strings encode the stacking sequences of the skin and the stiffener, whereas the third one encodes the geometric variable related to the stiffener web angle. The maximum number of plies for the skin laminate is equal to 24. Consequently, the first sub-string is composed of 12 genes due to the assumed symmetry of the stacking sequence. Similarly, the second sub-string, encoding the stiffener lay-up, is composed of 12 genes.

The ply code has an alphabet of cardinality four, where 1, 2 and 3 denote plies oriented at $0°$, $45°$, $90°$, and 4 indicates an empty ply. Following the approach of Soremekun et. al [33], the gene 2 is decoded alternatively as a $45°$ or $-45°$ ply.

The third sub-string adopts a binary encoding and is composed of four genes. The geometric variable, which varies between $0°$ and $25°$, can so assume discrete values with steps of $1.67°$.

5.2 Problem formulation

Goal of the optimization is the minimization of the structural weight with constraints regarding the pre-buckling stiffness, the buckling load and technological requirements. The

optimization problem is formulated as:

$$\begin{aligned} &\text{Minimize} \quad W \\ &\text{Subject to} \quad \begin{cases} K_{\text{pre}} > K_{\text{pre}}^{\text{ref}} \\ P_{\text{buck}} > P_{\text{buck}}^{\text{ref}} \\ \text{Design recommendations} \end{cases} \end{aligned} \tag{1}$$

where W is the weight of the panel, P_{buck} and $P_{\text{buck}}^{\text{ref}}$ are the buckling load and the reference value, while the terms K_{pre} and $K_{\text{pre}}^{\text{ref}}$ are the pre-buckling stiffness and the reference value. Constraints are introduced also to ensure that the optimal configuration meets some design recommendations [36], i.e.:

- Contiguity constraint: no more than four plies with the same orientation can be stacked together to avoid problems related to matrix cracking and delamination;
- Disorientation constraint: two consecutive ply orientations cannot differ for more than 45° in order to reduce edge delamination;
- Poisson's ratio mismatch: the difference of the equivalent Poisson's mismatch between adjacent laminates has to be taken below a maximum value of 0.1 to avoid delamination problems.

In the framework of genetic algorithms, the constrained problem of Eq. (1) is transformed into an unconstrained problem, and the fitness function is obtained as the product of the objective function, normalized with respect to a reference value $P_{\text{buck}}^{\text{ref}}$, and the penalty terms ξ_k. It becomes:

$$\text{fit} = \frac{W}{W^{\text{ref}}} \prod_{k}^{N_c} \xi_k \tag{2}$$

where N_c is the number of constraints. The expression for the penalty functions ξ_k depends on the type of constraint to be imposed, and distinction is made between structural and technological requirements.

The normalized violation of the generic k-th constraint Y_k is expressed as:

$$\Delta_k = 1 - \frac{Y_k}{Y_k^{\text{ref}}} \tag{3}$$

where the normalization is done with respect to a reference value Y_k^{ref}. In the present optimization, the generic terms Y_k are the pre-buckling stiffness and the buckling load. The penalty terms are built to vary from 0 to 1. When the constraint is respected, no penalty term is introduced and $\xi_k = 1$. On the other hand, the penalty term is less than 1 in presence

of a constraint violation. The adopted expression is:

$$\xi_k = \begin{cases} 1 & \text{if } \Delta_k \leq 0 \\ \dfrac{1}{(1+\Delta_k)^{\alpha}} & \text{if } \Delta_k > 0 \end{cases} \tag{4}$$

For the same level of constraint violation, the penalty term increases as the value of the exponent α is reduced, so determining the risk of obtaining configurations that do not respect the constraints. Higher values of the exponent tend to increase the reduction of the fitness function so limiting the ability of the genetic procedure to explore the design space. It is then necessary to find a good compromise between the advantages and the disadvantages associated to the choice of a given value of α. A preliminary assessment allowed to identify a value of $\alpha = 4$ as the most effective choice to guarantee the best reliability of the method. Concerning the technological requirements, the penalty terms related to the contiguity and the disorientation constraints are chosen as:

$$\xi_{\text{cp}} = \frac{1}{N_{\text{cp}}\gamma_{\text{tech}} + 1} \qquad\qquad \xi_{\text{dp}} = \frac{1}{N_{\text{dp}}\gamma_{\text{tech}} + 1} \tag{5}$$

where N_{cp} is the number of consecutive plies with the same angle of orientation in excess with respect to four. For instance, N_{cp} is 1 if the stacking sequence is characterized by five consecutive plies with the same orientation. If the constraint is respected, then N_{cp} is null and the penalty term is equal to 1.

The number of violations of the disorientation constraint is N_{dp}. According to industrial requirements, two consecutive plies oriented at 0° and 90° determine one violation. The scalar coefficient γ_{tech} is taken equal to 0.1.

The penalty term for the Poisson's mismatch $\Delta\nu$ between the skin and the stiffener laminates is:

$$\xi_{\text{pm}} = \begin{cases} 1 & \text{if } \Delta\nu \leq \Delta\nu^{\max} \\ 1/\left(1 + \gamma_{\text{tech}} \frac{\Delta\nu - \Delta\nu^{\max}}{\Delta\nu^{\max}}\right) & \text{if } \Delta\nu > \Delta\nu^{\max} \end{cases} \tag{6}$$

where $\Delta\nu^{\max}$ is the maximum allowed value.

It is observed that the stacking sequences generated during the optimization procedure are symmetric, but in general they can exhibit any degree of membrane anisotropy, i.e. the laminate can be not balanced. In order to guarantee that the laminate is symmetric and balanced, a repair procedure alternating the sign of the plies oriented at the same angle is implemented, and an additional penalty term is introduced. In particular, the fitness function is reduced by 75% if the skin of the panel is characterized by any degree of membrane anisotropy. On the other hand, a slight unbalancing of the stiffener lay-up has

not a significant effect on the buckling load of the panel and, for this reason, the penalty term is not introduced on the stiffener lay-up.

5.3 Optimization results

The reference values to normalize the fitness function of Eq. (2) are based on the Use Case panel configuration, which is taken as the starting design and whose lay-ups and stiffener geometry are reported in Table 4. The optimization aims to minimize the weight of the structure, while guaranteeing that the pre-buckling stiffness and the buckling loads are greater than 72.0 kN/mm and 55.7 kN, respectively.

An initial population of 40 individuals, randomly generated into the optimization domain, is considered. Good convergence to the optimal solution is found using one elite children, a crossover probability of 0.80 and a mutation probability of 0.05 for the bit flip, intra- and inter-laminar swap, ply addition, ply deletion and ply angle mutation. The crossover and mutation probabilities were defined on the basis of a preliminary tuning phase aimed to maximize the reliability on a simplified problem consisting in the buckling optimization of a simply supported panel. The maximum number of generations with no improvement is defined on the basis of past experience, and is taken equal to 20. The fittest individual is obtained after 63 generations. The stopping criterion considers a maximum number of generations with no improvement equal to 20, therefore the procedure terminates after 83 generations.

The optimal configuration is characterized by an angle ply skin with lay-up of $[\pm 45°/\pm 45°]_s$, while the lay-up of the stiffener is $[\pm 45°/0°_4/45°/0°]_s$. The web angle of the stiffener is 0°.

It can be observed that the skin lay-up is characterized by plies oriented at ±45°. On the other hand, ten of the sixteen plies composing the stiffener lay-up are oriented at 0°. The plies at 45° are inserted by the optimization procedure to avoid the violation of the contiguity constraint, thus reducing to four the number of consecutive plies at 0°.

The weight of the optimal configuration is 4.98 N, and is decreased by 3% with respect to the reference configuration. From Table 4 it can be also observed that the two constraints regarding the pre-buckling stiffness and the buckling load are respected. Worth of mention is the fact that an increase of 43% is observed in terms of the buckling load.

The optimal configuration is characterized by a stiffener pre-buckling stiffness of 64 kN/mm, approximately six times higher compared to the axial stiffness of the skin, which is 11 kN/mm.

The axial load carried by the structure is distributed inside the panel according to the

assumption of a common axial shortening, and consequently depends on the axial stiffnesses of the skin and the stiffener. In this case, the axial shortening at buckling is 1.06 mm, so the load carried by the skin is 11 kN, while the fraction of load carried by the stiffeners is 64 kN.

It is then concluded that the optimization automatically identifies a configuration where a subdivision of the structural requirements is observed. The skin lay-up is a soft-skin design, with a relatively low axial stiffness, and high stress and shortening at buckling. On the other hand, the stiffener lay-up is determined to provide the necessary axial stiffness, consequently increasing the load carried by the stiffeners at buckling.

The optimization totally consists of 3320 fitness evaluations. The pre-buckling stiffness is obtained from classical lamination theory in few fractions of a second, while the main effort is related to the evaluation of the buckling load. The average CPU time for the fitness evaluation is 0.9 s on a Core2 Duo 3.00 GHz with 2 GB of RAM and the total time required by the procedure is approximately 50 minutes. Considering that the CPU time for the eigenvalue finite element analysis of the optimal configuration is approximately 100 s, the time for an analogous optimization procedure based on finite element analyses can be estimated in about 92 h.

6 Conclusions

The paper discussed the development of a fast procedure for the design of composite stiffened panels based on a semi-analytical formulation for the structural analysis, and genetic algorithms for the optimization phase. The procedure was applied to the analysis and the optimization of the MAAXIMUS Use-Case fuselage panel, presenting also the comparison with finite element results.

The proposed tool represents an effective strategy to introduce buckling and post-buckling considerations since the preliminary design phases, limiting the risk of late and costly structural changes. The difference of the semi-analytical buckling loads compared to that one obtained using Abaqus is below 2%, and the comparison of the buckling shapes reveals a satisfactory level of accuracy. In terms of post-buckling response, good agreement is observed for the force-displacement curve, as well as the deformed shape and the stress distribution.

The main advantage of the proposed design fast tool consists in the possibility of reducing the computational effort with respect to the finite element method. The speed-up is achieved thanks to a more efficient analysis procedure based on few degrees of freedom and, in addition, geometric modeling and finite element meshing are not needed. In the proposed

example, the overall time for the optimization is approximately 50 *mins*, more than one hundred time faster in comparison to an analogous procedure based on finite element simulations.

The computational efficiency of the design procedure can be exploited in the context of multi-disciplinary design procedures, where different types of requirements are introduced, and where the evaluation of the buckling and post-buckling behaviour is demanded to the proposed tool. Similarly, the design procedure can be extended by coupling the analytical formulations with Abaqus or other finite element codes to obtain an hybrid optimization procedure.

Another advantage, related to the reduced computational time, consists in the possibility of studying larger design spaces. A high number of design variables can be easily handled, and different geometrical variables or unconventional lay-ups can be introduced in the optimization process.

7 Acknowledgements

The research leading to these results has been partially funded by the European Commission Seventh Framework Programme FP7/2007-2013 under grant agreement n° 213371, MAAXIMUS (www.maaximus.eu).

References

[1] LYNCH, C., MURPHY, A., PRICE, M. and GIBSON, A. The computational post buckling analysis of fuselage stiffened panels loaded in compression, *Thin-Walled Structures* 2004, **41**,(10), pp 1445–1464.

[2] LINDE, P., SCHULZ, A. and RUST, W. Influence of modelling and solution methods on the FE-simulation of the post-buckling behaviour of stiffened aircraft fuselage panels, *Composite Structures* 2006, **73**,(2), pp 229–236.

[3] LE TALLEC, P. Domain decomposition methods in computational mechanics, *Computational Mechanics Advances* 1994, **1**,(2), pp 121–220.

[4] CRESTA, P., ALLIX, O., REY, C. and GUINARD, S. Nonlinear localization strategies for domain decomposition methods: application to post-buckling analyses, *Computer Methods in Applied Mechanics and Engineering* 2007, **196**(8), pp 1436–1446.

[5] ALMROTH, B.O., STERN, P. and BROGAN, F.A. Automatic choice of global shape functions in structural analysis, *AIAA Journal* 1978, **16**,(5), pp 525–528.

[6] NOOR, A.K. and PETERS, J.M. Reduced basis technique for nonlinear analysis of structures, *AIAA Journal* 1980, **18**,(4), pp 455–462.

[7] BARRIÈRE, L., MARGUET, S., CASTANIÉ, B., CRESTA, P. and PASSIEUX, J.-C. An adaptive model reduction strategy for post-buckling analysis of stiffened structures, *Thin-Walled Structures* 2013, **73**,(0), pp 81–93.

[8] LITTLE, G.H. An efficient computer program for the large deflection analysis of rectangular orthotropic plates, *Computers & Structures* 1987, **27**,(4), pp 467–482.

[9] WEAVER, P.M. Approximate analysis for buckling of compression loaded long rectangular plates with flexural/twist anisotropy, *Proceedings of the Royal Society A: Mathematical, Physical and Engineering Science* 2006, **462**,(2065), pp 59–73.

[10] PEVZNER, P., ABRAMOVICH, H. and WELLER, T. Calculation of the collapse load of an axially compressed laminated composite stringer-stiffened curved panel - an engineering approach, *Composite Structures* 2008, **83**,(4), pp 341–353.

[11] QUATMANN, M. and REIMERDES, H.G. Computationally efficient analysis of the postbuckling behaviour of stiffened fuselage sections, In 53^{rd} *AIAA/ASME/ASCE/AHS/ASC Structures, Structural Dynamics and Material Conference* 2012, AIAA-2012-1961. Honolulu, HI.

[12] PAIK, J. and THAYAMBALLI, A. Buckling strength of steel plating with elastically restrained edges, *Thin-Walled Structures* 2000, **37**,(1), pp 27–55.

[13] QIAO, P. and SHAN, L. Explicit local buckling analysis and design of fiber-reinforced plastic composite structural shapes, *Composite Structures* 2005, **70**,(4), pp 468–483.

[14] BISAGNI, C. and VESCOVINI, R. Analytical formulation for local buckling and postbuckling analysis of stiffened laminated panels, *Thin-Walled Structures* 2009, **47**,(3), pp 318–334.

[15] FUJIKUBO, M. and YAO, T. Elastic local buckling strength of stiffened plate considering plate/stiffener interaction and welding residual stress, *Marine Structures* 1999, **12**,(9–10), pp 543–564.

[16] BYKLUM, E. and AMDAHL, J. A simplified method for elastic large deflection analysis of plates and stiffened panels due to local buckling, *Thin-Walled Structures* 2002, **40**,(11), pp 925–953.

[17] BUERMANN, P., ROLFES, R., TESSMER, J. and SCHAGERL, M. A semi-analytical model for local post-buckling analysis of stringer- and frame-stiffened cylindrical panels, *Thin-Walled Structures* 2006, **44**,(1), pp 102–114.

[18] BRUBAK, L. and HELLESLAND, J. Semi-analytical postbuckling and strength analysis of arbitrarily stiffened plates in local and global bending, *Thin-Walled Structures* 2007, **45**,(6), pp 620–633.

[19] MITTELSTEDT, C. Closed-form analysis of the buckling loads of uniaxially loaded blade-stringer-stiffened composite plates considering periodic boundary conditions, *Thin-Walled Structures* 2007, **45**,(4), pp 371–382.

[20] VESCOVINI, R. and BISAGNI, C. Buckling analysis and optimization of stiffened composite flat and curved panels, *AIAA Journal* 2012, **50**,(4), pp 904–915.

[21] BISAGNI, C. and LANZI, L. Post-buckling optimisation of composite stiffened panels using neural networks, *Composite Structures* 2002, **58**,(2), pp 237–247.

[22] MURUGAN, M.S., GANGULI, R. and HARURSAMPATH, D. Surrogate based design optimisation of composite aerofoil cross-section for helicopter vibration reduction, *Aeronautical Journal* 2012, **116**,(1181), pp 709–725.

[23] BUSHNELL, D. Optimum design of composite stiffened panels under combined loading, *Computers & Structures* 1995, **55**,(5), pp 819–856.

[24] KENNEDY, D. and FEATHERSTON, C.A. Exact strip analysis and optimum design of aerospace structures, *Aeronautical Journal* 2010, **114**,(1158), pp 505–512.

[25] DIACONU, C. and WEAVER, P.M. Approximate solution and optimum design of compression-loaded, postbuckled laminated composite plates, *AIAA Journal* 2005, **43**,(4), pp 906–914.

[26] HERENCIA, J., WEAVER, P.M. and FRISWELL, M. Optimization of long anisotropic laminated fiber composite panels with T-shaped stiffeners, *AIAA Journal* 2007, **45**,(10), pp 2497–2509.

[27] MAAXIMUS Project website. `http://www.maaximus.eu`.

[28] VESCOVINI, R. and BISAGNI, C. Two-step procedure for fast post-buckling analysis of composite stiffened panels, *Computers & Structures* 2013, **128**, pp 38–47.

[29] HYER, M. *Stress Analysis of Fiber-Reinforced Composite Materials*, pp 235-252. New York: McGraw-Hill, 1998.

[30] REDDY, J. *Mechanics of Laminated Composite Plates and Shells: Theory and Analysis*, pp 112-131. Boca Raton: CRC Press, 2004.

[31] FALZON, B. and STEVEN, G. Buckling mode transition in hat-stiffened composite panels loaded in uniaxial compression, *Composite Structures* 1997, **37**,(2), pp 253–267.

[32] NAGENDRA, S., JESTIN, D., GÜRDAL, Z., HAFTKA, R. and WATSON, L. Improved genetic algorithm for the design of stiffened composite panels, *Computers & Structures* 1996, **58**,(3), pp 543–555.

[33] SOREMEKUN, G., GÜRDAL, Z., HAFTKA, R. and WATSON, L. Composite laminate design optimization by genetic algorithm with generalized elitist selection, *Computers & Structures* 2001, **2**,(79), pp 131–143.

[34] FAGGIANI, A. and FALZON, B. Optimization strategy for minimizing damage in postbuckling stiffened panels, *AIAA Journal* 2007, **45**,(10), pp 2520–2528.

[35] ABAQUS version 6.13 *User's manual* 2013. Providence, RI, USA: SIMULIA World Headquarters.

[36] IRISARRI, F., BASSIR, D., CARRERE, N. and MAIRE, J. Multiobjective stacking sequence optimization for laminated composite structures, *Composites Science and Technology* 2009, **69**,(7-8), pp 983–990.

Table 1: Semi-analytical formulations.

Model	**Analysis**	**Solution type**	**Results**
Plate assembly	Linear	Eigenvalue	Buckling load Buckling mode
Elastically restrained	Nonlinear	Arc-length	Force - displacement curve Deformed shape Stress distribution

Table 2: Material elastic properties.

$E_{11}[MPa]$	$E_{22}[MPa]$	$G_{12}[MPa]$	ν_{12}
149000	10500	4200	0.3

Table 3: Ply strengths.

$X_t[MPa]$	$X_c[MPa]$	$Y_t[MPa]$	$Y_c[MPa]$	$S_{xy}[MPa]$
2500	1470	46	240	66

Table 4: Baseline and optimal configuration for curved stiffened panel.

	Baseline	Optimum
Skin lay-up	$[\pm 45^\circ/0^\circ/90^\circ/\mp 45^\circ]_s$	$[\pm 45^\circ/\pm 45^\circ]_s$
Stiffener lay-up	$[45^\circ/0^\circ/-45^\circ/0^\circ/90^\circ/0^\circ/-45^\circ/0^\circ/45^\circ]$	$[\pm 45^\circ/0^\circ_4/45^\circ/0^\circ]_s$
θ $[mm]$	10	0
P_{buck} $[kN]$	55.7	79.7
K_{pre} $[kN/mm]$	72.0	74.8
Weight $[N]$	5.12	4.98

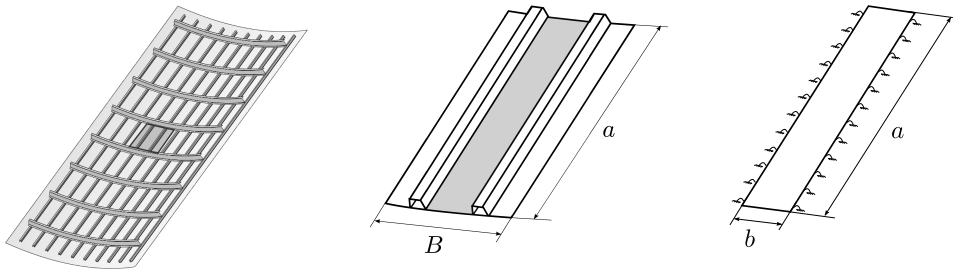

(a) (b) (c)

Figure 1: Different levels of approximation: a) multi-stiffener panel, b) plate assembly model for buckling analysis, c) elastically restrained skin for post-buckling analysis.

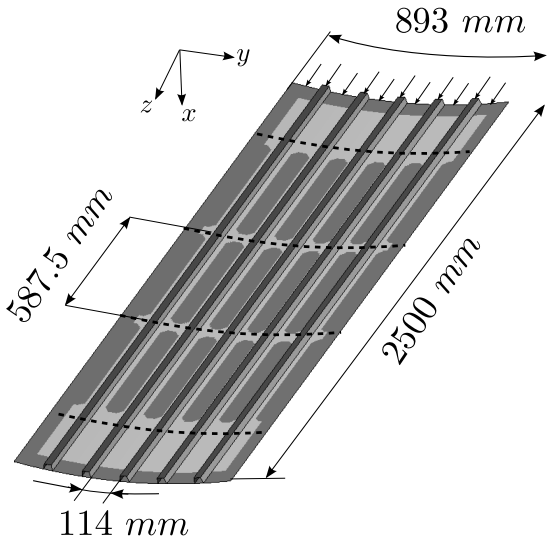

Figure 2: Use Case panel dimensions.

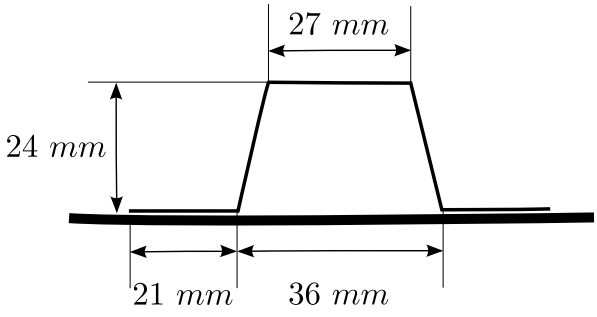

Figure 3: Details of the omega stiffener.

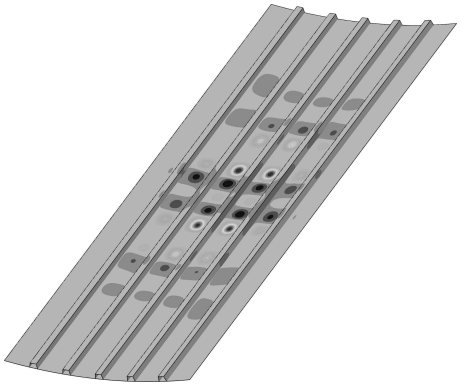

Figure 4: First buckling mode.

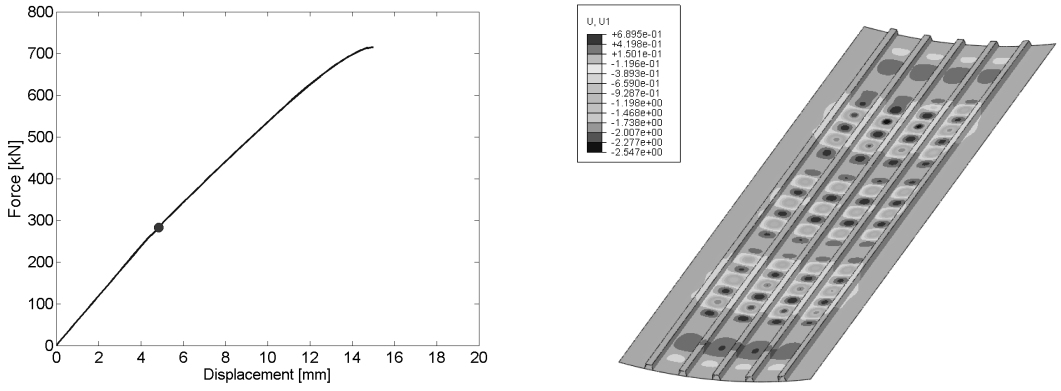

(a) (b)

Figure 5: Use Case panel: (a) load - shortening curve, (b) out of plane displacement at an imposed axial shortening of 4.88 mm and corresponding to the point indicated on the curve.

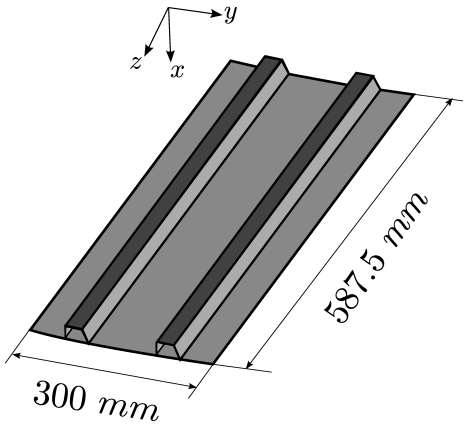

Figure 6: Dimensions of representative unit.

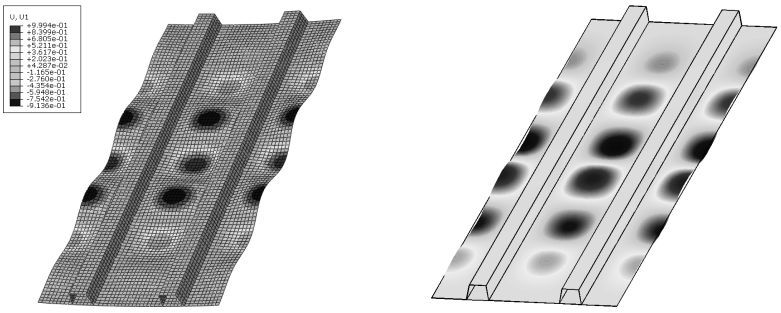

(a) (b)

Figure 7: Comparison between buckling mode shapes: (a) finite element, (b) semi-analytical.

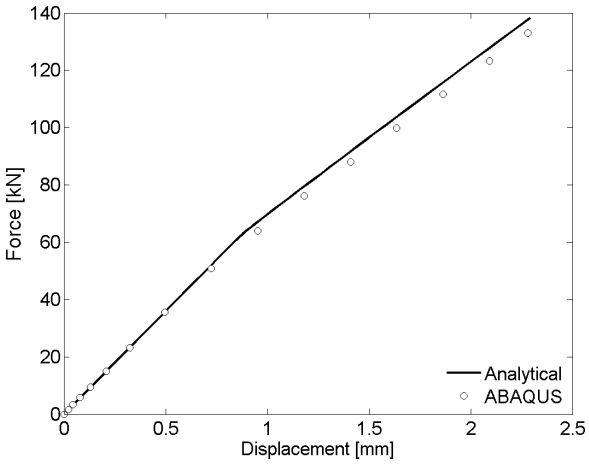

Figure 8: Load - shortening curve of the representative unit.

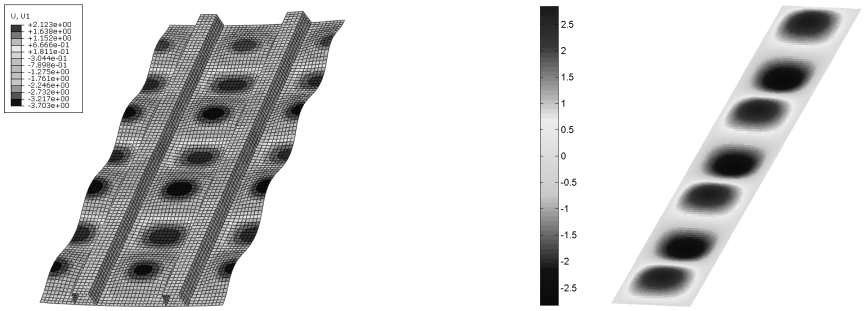

(a) (b)

Figure 9: Out of plane displacement contour at an imposed axial shortening of 2.3 mm: (a) finite element, (b) semi-analytical.

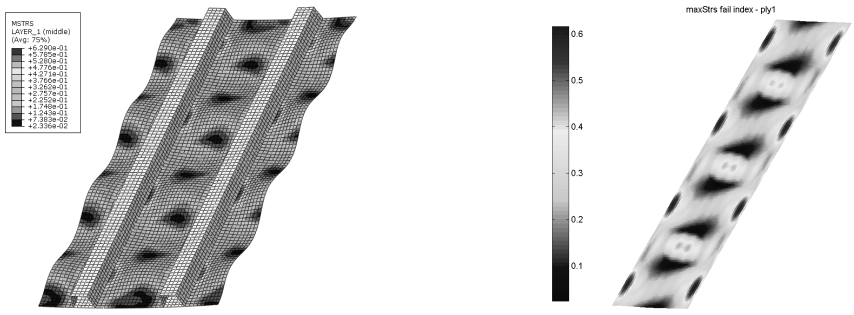

(a) (b)

Figure 10: Stress contour on ply 1 at an imposed axial shortening of 2.3 mm: (a) finite element, (b) semi-analytical.